

AN ENHANCED DFE FOR FBMC SYSTEMS OVER OQAM

E. RAJU¹ (M.TECH (VLSISD)).

T. CHAKRAPANI²(M.Tech,MISTE)

K.SUDHAKAR³(M.Tech (Ph.D),AMIE.)

rjgaru@gmail.com¹

tchakrapani57@gmail.com²

¹PG Scholar, VLSISD, St. JOHNS COLLEGE OF ENGINEERING & TECHNOLOGY, YEMMIGANUR.

²Associate Professor, Dept. of ECE, St. JOHNS COLLEGE OF ENGINEERING & TECHNOLOGY, YEMMIGANUR

³ Dept. of ECE, HOD, St. JOHNS COLLEGE OF ENGINEERING & TECHNOLOGY, YEMMIGANUR

ABSTRACT— *This paper proposes an upgraded decision feed-back equalizer (DFE) for filter bank multicarrier (FBMC) frameworks over offset quadrature amplitude modulation (OQAM) in view of a minimal mean square error (MMSE) basis. For each subcarrier, other than one feedforward (FF) channel and one feedback (FB) channel, we include two intercarrier interference (ICI)- suppressing channels, which feedback identified precursors separated from neighboring subchannels to improve ICI sup-pression within the sight of multipath channels. Our simulation results about show our proposition influences an extensive to enhancement contrasting and MMSE-DFE under an extreme ICI and ISI situation despite few extra costs computational complexity.*

Keywords—FBMC, OQAM, MMSE, decision feedback equalizer, intercarrier interference

I. INTRODUCTION

Nowadays, multicarrier (MC) systems are widely-known and attractive for wideband communications. The most well known system is orthogonal frequency-division multiplexing (OFDM), which encodes digital data on many narrowly divided frequency sub bands. The advantages of OFDM include simple equalization, channel estimation and the ability to combat severe channel conditions such as frequency selective fading [1]. OFDM recently has several applications, including digital television, audio broadcasting and 4G mobile communications. However, the orthogonality between OFDM subcarriers is maintained by adding cyclic prefixes (CP), which are the replicas of tailed signals of OFDM [2]. CP delimit successive OFDM symbols and bring about block transmission of OFDM, but sending CP certainly lowers power efficiency and data rate. In addition, sensitivity in frequency offset and out-of-

band interference are two other problems in OFDM. To cope with these problems of OFDM, some people discuss about FBMC that can be viewed as a practical alternative to OFDM. FBMC is also a MC system and subcarriers in filter banks are exponentially composed with longer impulse responses than OFDM signals [3]. Compared to rectangular prototype signals of OFDM, longer impulse responses of FBMC subcarriers enable FBMC to control non-adjacent orthogonality between FBMC subcarriers.

As a consequence, the well controlled orthogonality relieves out-of-band interference and frequency sensitivity of FBMC. Meanwhile, without redundant CP, FBMC can support higher power efficiency and throughput, and successive transmission can be achieved since block structure disappears. Additionally, to dodge ISI coming from overlapped FBMC signals and ICI between adjacent subcarriers, a novel OQAM scheme is used in FBMC. OQAM modulation staggers real parts and imaginary parts of QAM inputs to have adjacent subcarriers carry out-of phase half symbols simultaneously. In spite of it, when facing ISI channels, ISI and ICI still exist. In addition to additive white Gaussian noise (AWGN) at receivers, equalizer designs become a popular topic.

II. LITERATURE REVIEW

OFDM for Wireless Multimedia Communications

During the joint supervision of a Master's thesis "The Peak-to-Average Power Ratio of OFDM," of Arnout de Wild from Delft University of Technology, The Netherlands, we realized that there was a shortage of technical information on orthogonal frequency division multiplexing (OFDM) in a single reference. Therefore, we decided to write a comprehensive introduction to OFDM. This is the first book to give a broad treatment to OFDM for mobile multimedia communications.

Until now, no such book was available in the market. We have attempted to fill this gap in the literature.

Currently, OFDM is of great interest by the researchers in the Universities and research laboratories all over the world. OFDM has already been accepted for the new wireless local area network standards from IEEE 802.11, High Performance Local Area Network type 2 (HIPERLAN/2) and Mobile Multimedia Access Communication (MMAC) Systems. Also, it is expected to be used for the wireless broadband multimedia communications.

OFDM for Wireless Multimedia Communications is the first book to take a comprehensive look at OFDM, providing the design guidelines one needs to maximize benefits from this important new technology. The book gives engineers a solid base for assessing the performance of wireless OFDM systems. It describes the new OFDM-based wireless LAN standards; examines the basics of direct-sequence and frequency-hopping CDMA, helpful in understanding combinations of OFDM and CDMA. It also looks at applications of OFDM, including digital audio and video broadcasting, and wireless ATM. Loaded with essential figures and equations, it is a must-have for practicing communications engineers, researchers, academics, and students of communications technology.

An analysis of automatic equalizers for orthogonally multiplexed QAM systems

A simple structure of a per-channel automatic equalizer for an orthogonally multiplexed QAM system is proposed and the performance is analyzed. It is shown that a dual automatic equalizer with T/2-long tapped delay lines, where T is a period of individual baseband baud, can equalize not only the transmission channel distortions, but the timing deviations and demodulating carrier phase deviations. Despite its high efficiency, the orthogonally multiplexed QAM system has been regarded as overly costly. However, by using the dual automatic equalizer with fairly simple structure, the system is competitive with conventional single channel data transmission systems.

Notation

In this paper, we use the following notations for convenience. $(\bullet)^{(R)}$ and $(\bullet)^{(I)}$ are the real part and

imaginary part of a signal or a vector. j is $\sqrt{-1}$. A notation in bold is always a vector containing a finite-length sequence of symbols. I_N denotes the identity matrix of size N and 0_M and $0_{M \times N}$ represent an $M \times 1$ and an $M \times N$ zero matrix respectively, and mod is the modulo operation. $\lfloor \cdot \rfloor$ = the flooring function, $*$ is the convolution operation.

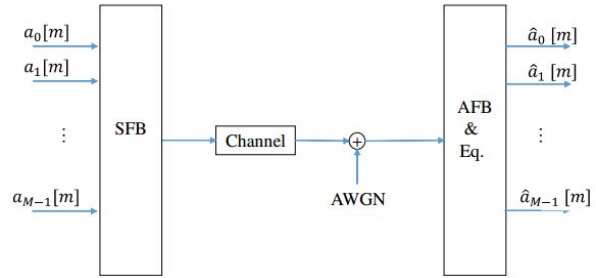


Fig. 1. Overview of FBMC

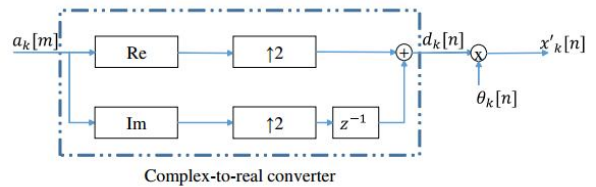


Fig. 2. OQAM pre-processing for an even k

III. FBMC/OQAM STRUCTURE

The core of FBMC systems is synthesis filter banks (SFB) and analysis filter banks (AFB) as Fig. 1 shows. The inputs $a_k[m]$ are complex QAM symbols to be carried by each subcarrier. To compose OQAM symbols, OQAM preprocessing is conducted in SFB, in which real parts and imaginary parts of QAM inputs are separated as shown in Fig. 2 for an even k. The order of transmission for half symbols depends on the subcarrier index, k. For odd-index subcarriers, imaginary parts are ordered ahead by placing the one-tap delay in Fig. 2 upside down. The staggered outputs are denoted by $d_k[n]$ and then the complex OQAM symbols and denoted by $x'_k[n] = \theta_k[n]d_k[n]$ with $\theta_k[n] = j^{(n+k)\text{mod}2}$, at the double rate of the inputs. Afterwards, the OQAM symbols are upsampled by M/2 and fed into a bank of M synthesis filters, whose impulse responses are designed by

$$h_k[l] = h_0[l]e^{j\frac{2\pi kl}{M}}, l = 0, \dots, KM - 1. \quad (1)$$

In (1), $h_0[l]$ is the KM-tap causal impulse response of a prototype filter, each subcarrier is shifted by 1/M in

frequency, and K is the overlapping factor. $h_0[l]$ needs designing as a Nyquist filter to provide an ISI-free transmission, and K is the ratio between the length of $h_0[l]$ and the averaged symbol duration. After filtered by SFB, all signals are composed into one waveform, up-converted into a radio frequency, and emitted.

IV. ENHANCED SUBCHANNEL MMSE-DFE WITH ICI SUPPRESSION

In the following, we consider a FBMC system with $K \geq 4$ such that the prototype filter possesses strong controllability in its stop-band. Accordingly, the interference from non neighboring subcarriers can be neglected. In this way, a subchannel model for the FBMC system can be drawn as Fig. 3 shows.

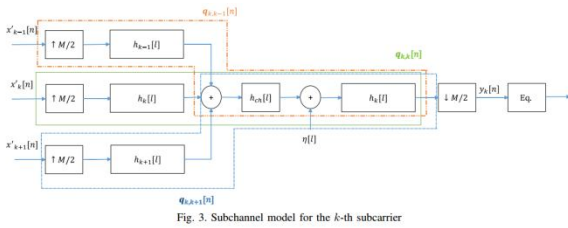


Fig. 3. Subchannel model for the k -th subcarrier

In Fig. 3, we define $q_{k,k+j}[n]$ ($j = -1, 0, 1$) as the effective ICI channels from the $k + j$ -th carrier to the k -th carrier, which can be formulated by

$$q_{k,k+j}[n] = \{h_{k+j}[l] * h_{ch}[l] * h_k[l]\}_{l=\frac{Mn}{2}}, n = 0, \dots, Q - 1, \quad (2)$$

where $Q = \lfloor \frac{2KM + L_{ch} - 2}{M/2} \rfloor$. Then, an received $N \times 1$ vector $y_k[n]$ can be analyzed in a matrix form,

$$\mathbf{y}_k[n] = \sum_{j=-1}^1 \mathbf{Q}_{k,k+j} \mathbf{x}'_{k+j}[n] + \mathbf{\Gamma}_k \mathbf{v}[l], \quad (3)$$

In (3), $\mathbf{Q}_{k,k+j}$ are the convolutional matrixes $\in \mathbb{C}^{N \times (L+1)}$ for $q_{k,k+j}[n]$, and $\mathbf{x}'_{k+j}[n]$ are $(L+1) \times 1$ transmitted symbol vectors, where $L = N - Q - 2$. The noise vector, $\mathbf{v}[l]$ is an $(KM + NM/2 - 1)$ -tuple AWGN vector with the k -th down sampling convolutional matrix, $\mathbf{\Gamma}_k$ resulting from $h_k[l]$. It is worth mentioning that the phases of elements in $\mathbf{x}'_k[n]$ depends on $k + n$,

$$\mathbf{x}'_k[n] = [d_k[n]\theta_k[n], d_k[n-1]\theta_k[n-1], \dots]^T \in \mathbb{C}^{L+1}. \quad (4)$$

The proposed structure of an enhanced sub channel MMSE DFE with ICI suppression is shown in Fig. 4.

Firstly, as with MMSE-DFE, one FF filter w_k and one FB filter $f_{k,k}$ are employed to filter down sampled symbols and detected symbols in the k -th sub channel respectively. In addition, the main extension of our proposal is the two ICI-suppressing filters, $f_{k-1,k}$ and $f_{k+1,k}$.

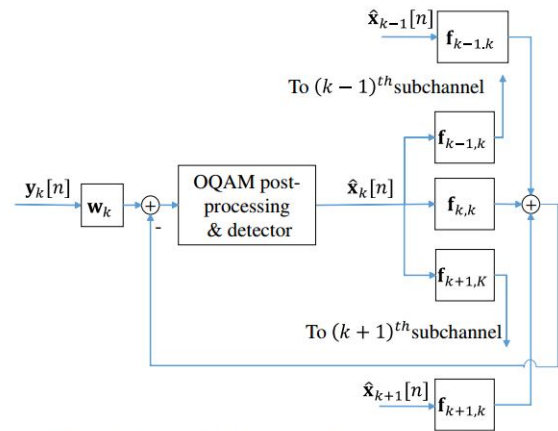


Fig. 4. Enhanced DFE with ICI suppressing filters

After subtraction, a detector and OQAM post-processing are followed to restore OQAM symbols and generate the latest FB inputs as Fig. 5 shows.

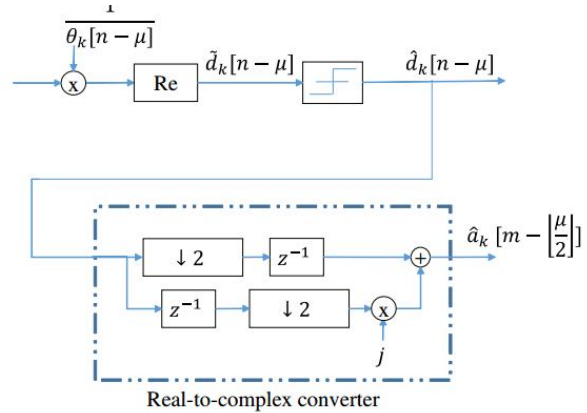


Fig. 5. OQAM pre-processing and detector

For an odd-index subcarrier, the multiplication with j is placed upside down to match the order of transmission. The input vectors of the FB filters, denoted by $\hat{\mathbf{x}}_{k+j}[n]$ with $B + 1$ tuples are real-valued vectors and defined by $\hat{\mathbf{x}}_{k+j}[n] = [d_{k+j}[n - \mu - 1], d_{k+j}[n - \mu - 2], \dots]^T \in \mathbb{R}^{B+1}$ (5)

where all the detections of precursors are assumed to be correct.

The value μ is a proper delay for equalization, which is relevant to the positions of maximum values of $h_{ch}[l]$ and $h_0[l]$ and can be optimized by simulation. In this paper, we set μ as a multiple of two but do not deal with the optimization. Instead, we use a fix value for μ through all simulations. Notably, when the detection of $d_{k+j}[n - \mu]$ is finished, the FB vectors are updated by pushing in $d_{k+j}[n - \mu]$.

Next, when estimating $d_k[n - \mu]$ for an even $n + k$, since the desired symbol is real-valued, the estimate, denoted by $\tilde{d}_k[n - \mu]$, can be expressed by

$$\begin{aligned} \tilde{d}_k[n - \mu] &= \left[\mathbf{w}_k^H \mathbf{y}_k[n] - \sum_{j=-1}^1 \mathbf{f}_{k+j,k}^H \hat{\mathbf{x}}_{k+j}[n] \right]^{(R)} \\ &= \mathbf{w}_k^{(R),T} \mathbf{y}_k^{(R)}[n] + \mathbf{w}_k^{(I),T} \mathbf{y}_k^{(I)}[n] - \sum_{j=-1}^1 \mathbf{f}_{k+j,k}^{(R),T} \hat{\mathbf{x}}_{k+j}[n]. \end{aligned} \quad (6)$$

As for an odd $(n + k)$, the estimate is given by

$$\begin{aligned} \tilde{d}_k[n - \mu] &= \left[\mathbf{w}_k^H \mathbf{y}_k[n] - \sum_{j=-1}^1 \mathbf{f}_{k+j,k}^H \hat{\mathbf{x}}_{k+j}[n] \right]^{(I)} \\ &= \mathbf{w}_k^{(R),T} \mathbf{y}_k^{(I)}[n] - \mathbf{w}_k^{(I),T} \mathbf{y}_k^{(R)}[n] + \sum_{j=-1}^1 \mathbf{f}_{k+j,k}^{(I),T} \hat{\mathbf{x}}_{k+j}[n]. \end{aligned} \quad (7)$$

In the above two equations, the real and imaginary parts of received symbols can be rewritten by

$$\begin{aligned} \mathbf{y}_k^{(R)}[n] &= \left[\sum_{j=-1}^1 \mathbf{Q}_{k,k+j} \mathbf{x}'_{k+j}[n] + \Gamma_k \mathbf{v}[l] \right]^{(R)} \\ &= \sum_{j=-1}^1 \mathbf{Q}'_{k,k+j} \mathbf{x}'_{k+j}[n] + \Gamma_k^{(R)} \mathbf{v}^{(R)}[l] - \Gamma_k^{(I)} \mathbf{v}^{(I)}[l], \quad (8) \\ \mathbf{y}_k^{(I)}[n] &= \left[\sum_{j=-1}^1 \mathbf{Q}_{k,k+j} \mathbf{x}'_{k+j}[n] + \Gamma_k \mathbf{v}[l] \right]^{(I)} \\ &= \sum_{j=-1}^1 \mathbf{Q}'_{k,k+j} \mathbf{x}'_{k+j}[n] + \Gamma_k^{(I)} \mathbf{v}^{(I)}[l] + \Gamma_k^{(R)} \mathbf{v}^{(R)}[l], \quad (9) \end{aligned}$$

where $\mathbf{x}_{k+j}[n] \in \mathbb{R}^L$ are obtained by shifting all j 's from $\mathbf{x}'_{k+j}[n]$ to $\mathbf{Q}_{k,k+j}$ to recover a staggered form matching with $\mathbf{x}_{k+j}[n]$, resulting in the matrixes $\mathbf{Q}'_{k,k+j}$ that contain the effect of $\theta_k[n]$, SFB, channels, AFB. For an even $k+n$, in all $\mathbf{Q}'_{k,k+j}$, the dimensions are unchanged but all the multiple-of-two-index columns are multiplied by j . Then, by defining the error as the distance between the estimate and the desired symbol, the MMSE criterion can be defined by

$$\left[\begin{matrix} \mathbf{w}_{k,o} \\ \mathbf{f}_{k,FB,o} \end{matrix} \right] = \arg \min_{\mathbf{w}_k, \mathbf{f}_{k,FB}} \mathbb{E}[|d_k[n - \mu] - \tilde{d}_k[n - \mu]|^2], \quad (10)$$

where

$$\mathbf{f}_{k,FB} = [\mathbf{f}_{k,k}^I, \mathbf{f}_{k-1,k}^I, \mathbf{f}_{k+1,k}^I]^T.$$

If $d_k[m]$ are wide sense stationary and uncorrelated, (6) and (7) can be optimized individually. Obviously, solving (6) only leads to the real part the MMSE solution of $\mathbf{f}_{k,FB}$ because the inputs of the FB filters are real, while solving (7) leads to the imaginary part.

Since we can prove that for a fixed k , the MMSE solutions for $\mathbf{w}'_{k,o}$ from (6) and (7) are the same, and for FB filters,

$$\begin{aligned} \mathbf{f}_{k,k,o}^{(R)}[n] &= (-1)^n \mathbf{f}_{k,k,o}^{(I)}[n] \quad \text{and} \\ \mathbf{f}_{k,k\pm 1,o}^{(R)}[n] &= (-1)^{(n+1)} \mathbf{f}_{k,k\pm 1,o}^{(I)}[n], \end{aligned}$$

the above operations on $\mathbf{Q}_{k,k+j}$ can be performed to obtain the following solutions in every sub channel. With the above analysis, we assume that the variance of AWGN is σ^2_η and $\mathbb{E}[|d_k[n]|^2] = \sigma_d^2/2$. By plugging (8) and (9), into (6) and (7) and with the orthogonality

$$\begin{aligned} \mathbb{E}[\epsilon_k[n] \mathbf{y}'_k[n]] &= \mathbf{0}_{2N+3(B+1)}, \\ \text{where } \epsilon_k[n] &= d_k[n - \mu] - \tilde{d}_k[n - \mu], \text{ and } \mathbf{y}'_k[n] = \\ &= \left[\mathbf{y}_k^{(R),T}[n], \mathbf{y}_k^{(I),T}[n], -\hat{\mathbf{x}}_k^T[n], -\hat{\mathbf{x}}_{k-1}^T[n], -\hat{\mathbf{x}}_{k+1}^T[n] \right]^T, \end{aligned}$$

and with the definition of

$$\mathbf{w}'_k = [\mathbf{w}_k^{(R),T}, \mathbf{w}_k^{(I),T}]^T \in \mathbb{R}^{2N},$$

the MMSE solution, (8) concludes with

$$\begin{aligned} \left[\begin{matrix} \mathbf{w}'_{k,o} \\ \mathbf{f}'_{k,FB} \end{matrix} \right] &= \\ &= \left[\begin{matrix} \mathbf{H}_k \mathbf{H}_k^T + \mathbf{M}_k \mathbf{M}_k^T + \mathbf{N}_k \mathbf{N}_k^T + \mathbf{R}_{\eta,k} & -\frac{\sigma_d}{\sqrt{2}} \mathbf{F}_k \mathbf{J}_\mu \\ -\frac{\sigma_d}{\sqrt{2}} (\mathbf{F}_k \mathbf{J}_\mu)^T & \frac{\sigma_d^2}{2} \mathbf{I}_{3(B+1)} \end{matrix} \right]^{-1} \left[\begin{matrix} \frac{\sigma_d}{\sqrt{2}} \mathbf{H}_k \mathbf{e}_\mu \\ \mathbf{0}_{3B+3} \end{matrix} \right] \end{aligned} \quad (11)$$

$$\begin{aligned} \text{with the following definitions, } \mathbf{F}_k &= [\mathbf{H}_k, \mathbf{M}_k, \mathbf{N}_k], \mathbf{H}_k = \\ &= \frac{\sigma_d}{\sqrt{2}} \begin{bmatrix} \mathbf{Q}'_{k,k} \\ \mathbf{Q}'_{k,k} \end{bmatrix}, \mathbf{M}_k = \frac{\sigma_d}{\sqrt{2}} \begin{bmatrix} \mathbf{Q}'_{k-1,k} \\ \mathbf{Q}'_{k-1,k} \end{bmatrix}, \mathbf{N}_k = \frac{\sigma_d}{\sqrt{2}} \begin{bmatrix} \mathbf{Q}'_{k+1,k} \\ \mathbf{Q}'_{k+1,k} \end{bmatrix} \\ \mathbf{R}_{\eta,k} &= \frac{\sigma_\eta^2}{2} \mathbf{\Gamma}_k \mathbf{\Gamma}_k^T, \mathbf{\Gamma}_k = \begin{bmatrix} \mathbf{\Gamma}_k^{(R)} & \mathbf{\Gamma}_k^{(R)} \\ \mathbf{\Gamma}_k^{(I)} & -\mathbf{\Gamma}_k^{(I)} \end{bmatrix}, \text{ and } \mathbf{J}_\mu \text{ is an} \end{aligned}$$

$(L + 1) \times (B + 1)$ matrix whose value is defined according to L , μ and B ,

$$\mathbf{J}_\mu = \begin{cases} [\mathbf{0}_{(\mu+1) \times B'} \mathbf{I}_{B'} \mathbf{0}_{(L-B'-\mu) \times B'}]^T, & L - \mu > B', \\ [\mathbf{0}_{(\mu+1) \times B'} \mathbf{I}_{B'} \mathbf{0}_{(L-\mu) \times (B'+\mu-L)}]^T, & L - \mu < B', \\ [\mathbf{0}_{(\mu+1) \times B'} \mathbf{I}_{B'}]^T, & L - \mu = B', \end{cases} \quad (12)$$

where $B' = B + 1$.

V PERFORMANCE EVALUATIONS

In this section, to contrast our proposal and the former works, including one-tap, MMSE, and MMSE-DFE, we discuss their structural configurations and corresponding computational complexity first. Then we show our simulation results to confirm their effectiveness and performance.

TABLE I

COMPLEXITY ANALYSIS. DESIGN COMPLEXITY AND PROCESSING COMPLEXITY FOR EACH DESIGN

	Design Complexity	Processing Complexity
One-tap	0	2
MMSE	$O(N^2)$	$2N$
MMSE-DFE	$O(N^2 + NB + B^2)$	$2N + B + 1$
Our proposal	$O(N^2 + NB + B^2)$	$2N + 3B + 3$

A. Complexity analysis

Firstly, all of the equalizers are equipped with a FF filter. A one-tap equalizer provides the simplest solution with an unit-tap filter; in contrast, the other three equalizers supply an N-tap FF filter. MMSE-DFE and our enhanced DFE have extra FB structure to combat ISI and ICI. MMSE-DFE has one $B + 1$ -tap FB filter and our proposal has three. Secondly, since only one phase is cared in each detection, we consider processing complexity in terms of the number of real multipliers (RMUX) demanded by each design. A FF and a FB filter need $2N$ and $B + 1$ RMUX respectively. In contrast with MMSE-based equalizers, matrix computation is waived and only two RMUX are needed in an one-tap equalizer. Table I concludes the above analysis.

B. BER performance

Next, we evaluate the performance of different equalizers in terms of BER. The parameter settings of the system are as follows: $M = 128$ and QPSK-modulated. The prototype filter is a root raised cosine filter with roll-off factor = 0.5 and the overlapping factor $K = 4$, which is a nearly Nyquist filter, such that its non-adjacent ICI can be negligible.

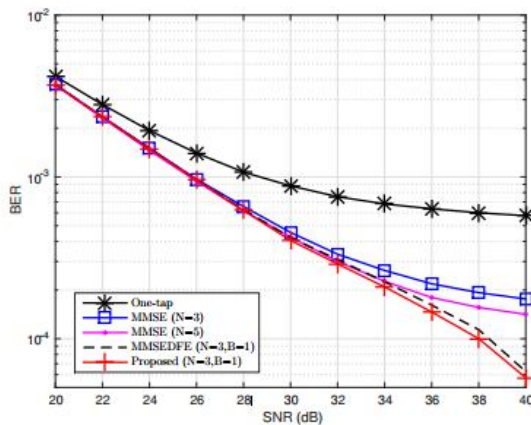


Fig. 6. BER curves of different equalizers with a varying SNR, $\tau_{max} = 25$ and $\tau_{rms} = 2$

Fig. 6 contrasts the performance of one-tap, MMSE, MMSE-DFE, and our proposal as a function of SNR. The maximal delay spread, τ_{max} of the channel is 25-tap and the root-mean-square (RMS) delay spread, τ_{rms} is two-tap both at the same rate of 1. Firstly, we set all the FF filters threetap in MMSE, MMSE-DFE and our proposal, and FB filters are two-tap (i.e., $B = 1$). As can be

seen, all algorithms perform almost the same in the low SNR region (around 20 dB). On the other hand, at the BER of 2×10^{-4} , the ISI-suppressing filter brings a three-dB gain in SNR.

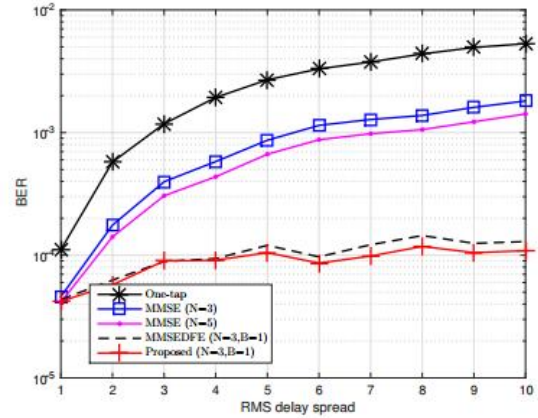


Fig. 7. BER curves of different equalizers in multipath channels with a varying τ_{rms} and SNR = 40 dB $\tau_{max} = 25$

The main reason for the limited improvement is that ISI and ICI dominate at a high SNR and the power of one FF filter of MMSE is insufficient to combat ISI and ICI. With the help of one FB filter in MMSE-DFE, ISI can be suppressed but residual ICI still remains. Our proposed ICI suppressing filters are proven capable of coping with residual ICI. In Fig. 7, we vary τ_{rms} from one tap to 10 taps and fix the SNR = 40 dB and $\tau_{max} = 25$. With a longer delay spread (that is, highly frequency selective), the effect of ICI and ISI becomes more outstanding as mentioned. In this simulation, we can see the three MMSE-based equalizers have similar performance at a short τ_{rms} . Contrarily, our proposal outperforms the other three equalizers when τ_{rms} is increased. For the above results, we can conclude our proposed scheme can be seen as a powerful equalizer in a highly selective channel or at a high SNR.

VI. CONCLUSION

In conclusion, the issue of FBMC/OQAM under ISI channels is explored. Next, utilizing MMSE-DFE as a model, we propose an upgraded DFE with two ICI smothering channels included and after that enhance these channels in view of the MMSE rule. Under a error free detection assumption, the expository outcome can be gotten. In our simulation, the change

from the two ICI suppressing channels is impressive in a high SNR region and on highly particular divert conditions despite an additional slight weight in calculation. In a non-static channel, the channel coefficients require refreshing with the end goal that outline unpredictability turns out to be more huge. Effective versatile DFE outlines like are important in progressively transmission of FBMC/OQAM. Additionally, wrong FB signals require be thought about. A further change can be normal when a particular choice criticism strategy is found. Direct estimation in FBMC is likewise another issue.

REFERENCES

- [1] R. Nee, and R. Prasad, "OFDM for Wireless Multimedia Communications", Artech House, 2000.
- [2] B. Farhang-Boroujeny, "OFDM Versus Filter Bank Multicarrier", IEEE Signal Processing Magazine, vol. 28, pp. 92-112, May 2011.
- [3] B. Farhang-Boroujeny, "Cosine Modulated and Offset QAM Filter Bank Multicarrier Techniques A Continuous-Time Prospect," EURASIP Journal on Advances in Signal Processing, pp. 6, Jan 2010.
- [4] V. Ari, B. Maurice, and H. Mathieu, "WP5: Prototype filter and filter bank structure", PHYDYAS-Physical layer for DYnamic AccesS and cognitive radio, Jan 2009.
- [5] B. Hirosaki, "An analysis of automatic equalizers for orthogonally multiplexed QAM systems," IEEE Transactions on Communications, 28(1). pp. 73-83, Jan. 1980.
- [6] S. Nedic and N. Popvic, "Per-bin DFE for advanced OQAM-based multicarrier wireless data transmission systems," Broadband Communications, 2002. Access, Transmission, Networking. 2002 International Zurich Seminar on, pp. 38-1, Feb. 2002.
- [7] D. S. Waldhauser, L. G. Baltar and J. A. Nossek, "MMSE subcarrier for filter bank based multicarrier systems," Proc. IEEE 9th Workshop on Signal Processing Advances in Wireless Communications, pp.525-529, July 2008.
- [8] A. Ikhlef and J. Louveaux, "An enhanced MMSE per subchannel equalizer for highly frequency selective channels for FBMC/OQAM systems," Proc. IEEE 10th Workshop on Signal Processing Advances in Wireless Communications, pp. 186-190. June 2009.
- [9] L. G. Baltar, D. S. Waldhauser and J. A. Nossek, "MMSE subchannel decision feedback equalization for filter bank based multicarrier systems," Proc. IEEE

International Symposium on Circuits and Systems pp. 2802-2805, May 2009.

BIOGRAPHIES:

1.E.RAJU WAS BORN IN 1994 IN VARKUR VILLAGE,KURNOOL,A.P. COMPLETED DIPLOMA ECE IN GOVT POLYTECHNIC COLLEGE ADONI, COMPLETED B.TECH IN ST.JHONS COLLEGE OF ENGG & TECHNOLOGY,YEMMIGANUR AND NOW I AM STUDYING M.TECH VLSISD IN ST.JHONS COLLEGE OF ENGG & TECHNOLOGY ,YEMMIGANUR.

E.RAJU, M.TECH ECE (VLSISD).



2. T.CHAKRAPANI WAS BORN IN 1975 IN PRODDATUR,KADAPA, A.P.AFTER COMPLETION OF DIPLOMA IN ECE WORKED AS DIGI COM SERVICE ENGINEER. B.Tech COMPLETED IN JNTU HYDERABAD IN 2001,WORKED AS GRADUATE APPRENTICE IN ORDINANCE FACTORY,MINISTRY OF DEFENCE,HYD., COMPLETED M.Tech IN SIDDHARTHA ENGG COLLEGE AT VIJAYAWADA IN 2005,(SPECIALIZATION IN MICROWAVE ENGG). FROM 2005 TO TILL DATE WORKING IN ST.JHONS COLLEGE OF ENGG &TECH,YEMMIGANUR. WORKING AS ASSOCIATE PROFESSOR ,T&P OFFICER,PROJECT CO -ORDINATOR FOR B.Tech AND M.Tech STUDENTS AND GUIDED MANY M.Tech & B.Tech PROJECTS IN VARIOUS DISCIPLINES OF ECE.AND PUBLISHED MANY PAPERS IN NATIONAL AND INTERNATIONAL JOURNALS WITH HIS STUDENTS.ATTENDED MANY WORKSHOPS AND CONFERENCES IN VARIOUS AREAS IN COMMUNICATION ENGG. T.Chakrapani M.Tech,MISTE ASSOCIATE PROFESSOR of ECE Department, ST.JHONS COLLEGE OF ENGG & TECHNOLOGY ,YEMMIGANUR.

T.CHAKRAPANI M.TECH,MISTE

